

STUDY INTO MECHANICAL PROPERTIES AND DESIGN METHOD OF LARGE CABLE SOCKETS

By Tsutomu KOMURA*, Katsuya WADA**, Haruo TAKANO***
 and Yoshifumi SAKAMOTO****

The mechanical properties of large sockets in which cable terminals are secured with zinc-copper alloy were studied and a design method for this type of socket was proposed. When sockets for large cables are designed by applying the conventional design method, one inevitable consequence is insufficient wall thickness, which leads to large deformations of the socket itself under the cable breaking load. Since the mechanical properties of a large socket are different from those of small one, the conventional design method is inapplicable to such a socket. The new design method studied in this work introduces the concept of rigidity for ultimate strength into large socket design.

Keywords: cable, socket, ultimate strength, cable-stayed bridge

1. INTRODUCTION

The cable terminals of cable-stayed bridges and suspension bridges are generally anchored by sockets. A zinc-copper alloy (Zn 98 Cu 2) is generally used in the various types of socket^{1), 2)}.

The main mechanical properties required of the cables, including the sockets, are high static strength, high modulus of elasticity and fatigue strength corresponding to the particular application. With respect to the static strength in particular, a design is generally required such that the socket strength is not less than the strength of cables^{1), 2)}.

The design of sockets used for various types of bridge cable, including the parallel wire strands of suspension bridges, takes into consideration the extraction resistance of the wires, the allowable compressive forces on the zinc-copper alloy as determined mainly from the creep properties and the stress in the socket cone. The hoop stress generated on the internal surface of the socket under the design load must be less than the allowable tensile stress of the socket material³⁾. This principle is the basis of socket cone design.

In recent years, cables have inevitably become larger, in step with the increase in scale of cable-stayed bridges, for example, the Yokohama Bay Bridge has adopted one of the largest cables in its construction. It is 175 mm in diameter with 421 zinc-coated steel wires, each 7 mm in diameter. The breaking load of the cable is 2 592 tf (25 419 kN) which makes it about 6-7 times stronger than the parallel wire strands

* Member of JSCE, Councilor, Metropolitan Expressway Public Corp. (1-4-1 Kasumigaseki, Chiyoda-ku, Tokyo 100)

** Member of JSCE, Senior Expert Staff Engineering Department, ditto.

*** Member of JSCE, Deputy Head of Special Structural Design Div., Kanagawa Construction Bureau, ditto. (2-25 Masago-cho, Naka-ku, Yokohama 231)

**** Member of JSCE, Manager, Bridge Engineering and Construction Div. Nippon Steel Corp. (2-6-3 Otemachi, Chiyoda-ku, Tokyo 100-71)

commonly used in suspension bridges. There are many unknowns in the mechanical properties of structures containing sockets in the case of such a large diameter cable. In particular, it remains unclear whether the conventional method of design guarantees sufficient anchorage strength to support the breaking load of such a large diameter cable.

Accordingly, the authors carried out tensile breaking tests and model tests using the largest type of cable anchored in a socket to examine the mechanical properties of large sockets. As a result, the mechanical properties of large-diameter cables such as breaking load and socket strength were found to be different from the those of conventional small diameter cables. In response to this, new methods of design for large sockets were studied using elasto-plastic analysis. This led to a clarification of the problems concerning the conventional socket design method. In addition, it was discovered that limits on the deformation of the socket, and hence its rigidity, which had been completely disregarded in the conventional design method, must be introduced to satisfy the ultimate conditions.

This paper describes the design methodology developed for large sockets based on the results of a series of tests and on the analytical studies mentioned above.

2. CONVENTIONAL SOCKET DESIGN METHOD

(1) The method of design²⁾

The design criteria applied to conventional sockets anchored with zinc-copper alloy (Zn 98 Cu 2) are as follows :

a) Length of the alloy cone is determined by two main conditions. The maximum pressure σ_M , calculated by Eq. (1) must not be greater than the allowable compressive stress as determined primarily from the creep properties. In addition, the bond length l_b must be sufficient to prevent the extraction of a single wire.

$$\sigma_M = \frac{T}{A} \cdot \frac{\cos \rho}{\sin(\theta + \rho)} \quad (1)$$

Where, T : Cable design load, A : Effective contact area of the zinc-copper alloy cone, θ : Taper angle of socket interior, ρ : Angle of friction between the internal surface of the socket and the outer surface of the zinc-copper alloy cone.

$$l_b = \frac{d \cdot \sigma_u}{4 \cdot B} \quad (2)$$

Where, d : Diameter of wire (mm), σ_u : Tensile strength of wire (kgf/mm²), B : Adhesion between zinc-copper alloy and wire (kgf/mm²).

The casting length is decided by the larger of the two values calculated using Eqs. (1) and (2). When designing sockets of larger dimensions, Eq. (1) is usually predominant.

b) Wall thickness of socket cone³⁾

Assuming that the socket cone is a thick-walled circular pipe on which a uniform internal pressure σ_M is acting, the thickness of the wall is determined such that the hoop stress σ_θ on the internal surface of the socket computed from Eq. (3) is not greater than the allowable stress.

$$\sigma_\theta = \sigma_M \cdot \frac{b^2 + a^2}{b^2 - a^2} \quad (3)$$

where, σ_M : Internal pressure, a : Average internal radius, b : Average external radius.

Fig.1 shows a zinc-copper filled socket.

(2) Limitations of the method⁴⁾

The following two limitations of the conventional design method arise when it is applied to large sockets.

a) In checking the stress

A three-axis stress acts on the socket cone, consisting not only of the hoop stress but also a radial stress and a stress in the direction of the cable axis. To check the stress using only Eq. (3) is therefore

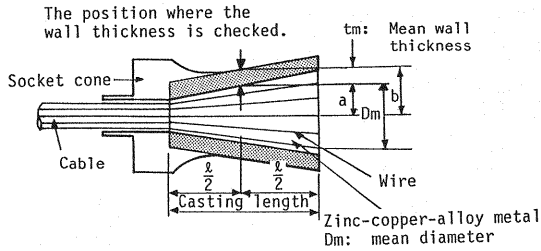


Fig. 1 Zinc-copper-alloy filled socket.

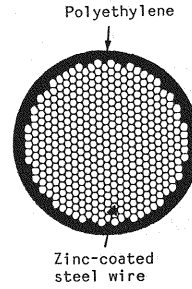
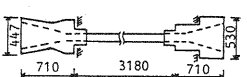
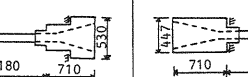
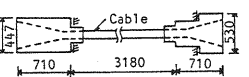
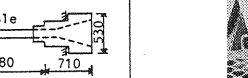


Fig. 2 Cross-section of cable (7 φ×421).

Table 1 Test specimens for the tensile breaking test.

Case	1	2	3	4
Combina- tion of socket	Thin walled front-bearing type & rear-bearing type	Thin walled front-bearing type & rear-bearing type	Thick walled front-bearing type & rear-bearing type	Thick walled front-bearing type & rear-bearing type
Size of specimen	Thin walled front-bearing type 	Rear-bearing type 	Thick walled front-bearing type 	Rear-bearing type 
Cable	Size; 7 mmφ x 421 wires		Size; 7 mmφ x 421 wires	

Note: Material quality of socket; S45C

(Unit: mm)

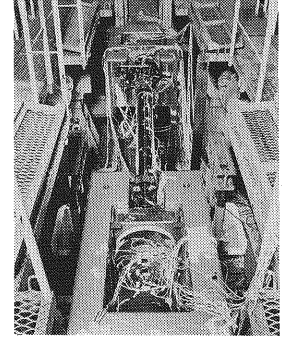


Photo 1 Test arrangement.

inadequate, and if the combined stress due to the three components is evaluated using a formula of combined stress, it is often found that the total stress is beyond the allowable stress even though the hoop stress is within limits.

b) In the ultimate condition

The conventional method of design does not take into account the strength required under ultimate conditions. As long as the design aims to guarantee against breakage, it is necessary to consider the ultimate strength beyond the elastic range, but the conventional method of elastic design lacks consideration of this point.

Although these problems do exist, conventional sockets for small-diameter cables, such as the parallel strands of suspension bridges, etc. do have sufficient static strength and no particular problems have occurred^{(5), (6)}.

3. TESTS ON THE MECHANICAL PROPERTIES OF LARGE SCALE SOCKETS

(1) Tensile breaking test on large-diameter cable

a) Summary of the test

This tensile breaking test was carried out with the emphasis on understanding the conditions at the breaking load of a large diameter cable corresponding to the socket type shown in Table 1. An 8 000 tf (78 453 kN) tensile strength testing device was used. Photo 1 is an overall view of the test apparatus.

Sockets can be classified into the front-bearing type and the rear-bearing type. Cables in each case were fixed by both types shown in Table 1. The front-bearing types used in the tests were thin walled sockets produced by the conventional design method and thick walled sockets with a larger wall thickness than calculated by the conventional method. The rear-bearing types were of the same size in each case. The local stress at the corner of the rear-bearing type was checked by F. E. M. (Finite Element Method). Tensile tests on the socket material indicated that its yield stress σ_y was 42 kgf/mm² (412 MPa).

The cable used in the test was the largest one in use, as used for the Yokohama Bay Bridge, and consists

Table 2 Results of the tensile breaking test.

Case		1	2	3	4
Tensile strength of wire		167.0 kgf/mm ²	167.0 kgf/mm ²	173.5 kgf/mm ²	173.5 kgf/mm ²
Break- ing load	Specified value A*	2,592 tf	2,592 tf	2,592 tf	2,592 tf
	Calculated value B**	2,706 tf	2,706 tf	2,811 tf	2,811 tf
	Measured value C	2,610 tf	2,598 tf	2,771 tf	2,743 tf
C/A		1.01	1.00	1.07	1.06
C/B		0.96	0.96	0.99	0.98
Slip- page	Front-bearing type socket	48 mm	56 mm	8 mm	11 mm
	Rear-bearing type socket	11 mm	8 mm	8 mm	7 mm
Failure position		Concentrated on the front face of zinc-copper alloy	Concentrated on the front face of zinc-copper alloy	Parallel section of wires	Parallel section of wires
Elongation of cable at breaking load		3.5%	2.8%	6.8%	5.5%

Notes: *; 160.0 kgf/mm²(1,569 MPa) x cross-sectional area of cable
 **; tensile strength of wire x cross-sectional area of cable

1 tf = 9.807 KN
 1 kgf/mm² = 9.807 MPa

of 421 zinc-coated steel wires 7 mm in diameter (hereafter referred to as "wires"), which were stranded in parallel and twisted only to the extent that the tensile strength and the modulus of elasticity were not affected.

b) Test results

Table 2 shows the results of these tests including the cable breaking load, the position and the elongation of the cable failure. In cases 1 and 2 where a thin walled front-bearing socket and a rear-bearing socket were used, although the measured load at which the cable failed (C in Table 2) satisfied the specified value (A in Table 2), these were within a small margin of the lower limit. Slippage in the thin walled front-bearing socket was about 50 mm. In addition, the failures were concentrated in a particular location near the front face of the zinc-copper alloy casting inside the socket only in the thin walled front-bearing type, a breakage pattern that has not been seen in conventional small-diameter cables before. The cable breaking strength efficiency (C/B in Table 2) was reduced by about 4 %. On the contrary, in cases 3 and 4 where thick walled rear-bearing sockets were used, slippage in the thick walled front-bearing type was about 10 mm and the cable breaking strength efficiency was only reduced by 1-2 %. Slippage in the rear-bearing sockets was about 10 mm in each case.

Fig. 3 shows the strain in the direction of the axis and around the circumference of the socket as measured using biaxial gages. In the case of the thin walled front-bearing type of socket, most of the external surface plasticized when the breaking load was applied and deformation (bulging of the radius) of the socket reached about 5-6 mm. This led to slippage of the zinc-copper alloy by about 50 mm in the direction of the cable.

On the other hand, in the case of the thick walled front-bearing socket and the rear-bearing socket, although local plasticization of the bearing surface occurred under the breaking load, most of the external surface of the socket stayed within the elastic region and deformation of the socket was extremely small, i.e. about 0.2-0.3 mm, and slippage of the zinc-copper alloy was small, i.e. about 10 mm.

The position at which the cable broke was scattered along the portion where the wires are parallel in the cable, and there were no concentrations at particular locations in the socket.

The elongation of the cable at the breaking load was 2.8-3.5 % in cases 1 and 2 where a thin walled front-bearing socket was used, about half the elongation of the wire (5-7 %) and below its specified value of 4 %. On the contrary, in cases 3 and 4 where a thick walled front-bearing socket was tested, the value was 5.5-6.8 %, which is close to the elongation of the wires and satisfied the specified value.

After the test was completed, the thin walled socket was dismantled and the cable failure position was investigated. It was found that the wires near the front face of the zinc-copper alloy in the socket had undergone local bending deformation due to squeezing around the point where the breakages were concentrated. The broken ends of the wires were similar to cup and cone shaped surfaces which is typical indication of ordinary ductile failure.

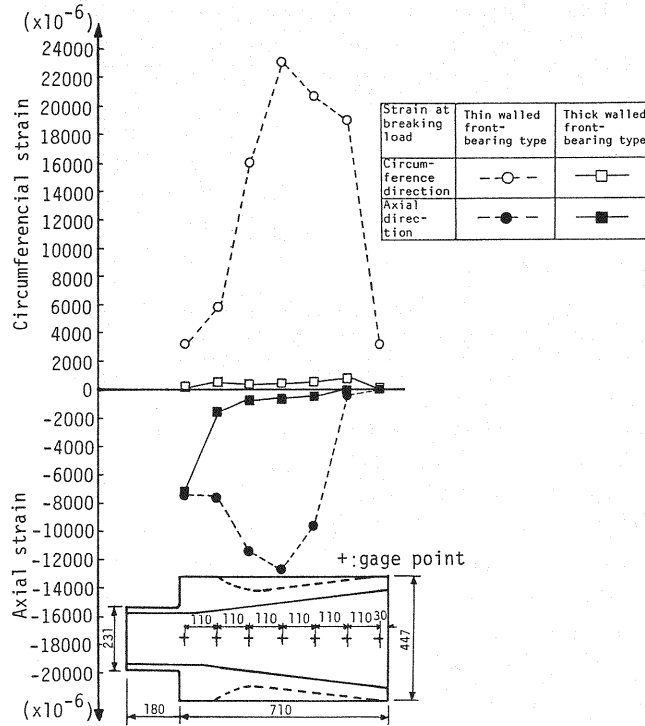


Fig. 3 Strain distribution on the external face of the socket.

(2) Model tests

Assuming from these results that there was a close relationship between the amount of slippage in the alloy cone, the cable failure pattern, and the breaking strength efficiency, a further test of tensile failure was conducted using models with small diameter cables (one model in which the slippage was intentionally increased by varying the wall thickness of the socket and one in which no such modification was made). It can be seen that where the ratio of the mean wall thickness t_m and the mean diameter of the alloy cone D_m , t_m/D_m (defined as "socket rigidity") was small, the amount of slippage increased and the failure positions tended to concentrate in a particular location inside the socket, lowering the breaking strength efficiency. On the contrary, when the socket rigidity t_m/D_m was larger than a certain value it was confirmed that no such phenomenon occurred.

As originally assumed, a close relationship exists between the amount of slippage in the zinc-copper alloy cone and the strength characteristics of the cable. Fig. 4 shows this relationship. The failure of the wires took place in the outermost layer of the cable in most cases.

(3) Factors affecting the cable breaking strength

On the basis of the tests, the factors possibly affecting the breaking strength can be classified into a)-d) below.

a) Factors related to phenomena occurring when the cable breaks

As the deformation of the socket increases, the

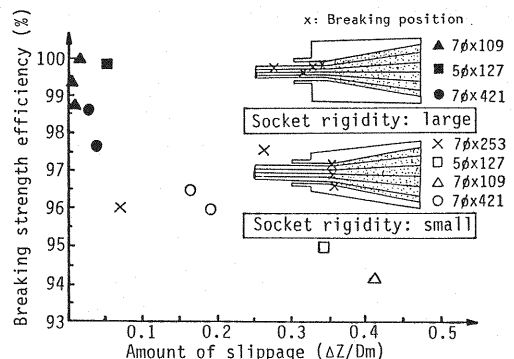


Fig. 4 Relationship between breaking strength efficiency and amount of slippage.

Table 3 Results of small diameter parallel wire cable breaking test.

Test specimen N: Number of specimens	Breaking load A (specified value) (tf)	Measured breaking load C (mean) (tf)	C/A	$\alpha = \frac{\text{Measured breaking load}}{\sigma_B \times \text{Cross-sectional area of cable}} \times 100(\%)$ where, σ_B : tensile strength of wire (mean value)	
				σ_B (kgf/mm ²)	α (%)
5.04 x 91 N=48	290	304.8	1.05	167	100
5.17 x 127 N=2	427	454.0	1.06	168	100
5.00 x 169 N=4	520	548.4	1.05	166	99.6
5.00 x 217 N=1	682	695	1.02	166	98.3
5.00 x 271 N=1	851	892	1.05	168	99.8
7.00 x 91 N=1	560	580	1.04	165	100
7.00 x 109 N=3	671	712.7	1.06	171	99.4
7.00 x 109 N=6	671	723.0	1.08	173	99.6

1 tf=9.807 kN, 1 kgf/mm²=9.807 MPa

amount of slippage in the zinc-copper alloy cone rises and the breaking position of the cable concentrates inside the socket, reducing the breaking strength efficiency. It is clear that a lower rigidity t_m/D_m makes the socket easily deformable. It is therefore clear that the phenomenon would not occur if the socket rigidity was sufficiently high to control this deformation.

To explain these phenomena, the following mechanisms may be considered: The lateral force on the wires from the internal face of the socket grows rapidly from a low value as the slippage in the alloy cone increases. As a result, the strain in a direction perpendicular to this lateral pressure, i. e. along the axis of the wires, can be expected to be larger. In addition, since the wires are subjected to local bending deformation followed by squeezing, bending strain and shear strain are concentrated in that area. These two mechanisms strain the wire to its elongation limit and ductile failure occurs⁹⁾. This explains the cup and cone appearance of the broken wire ends seen in the tests.

b) Factors resulting from increased cable diameter

Table 3 shows data obtained in breaking tests on small diameter cables carried out by the authors and also taken from references⁷⁾. It can be seen from this data that the reduction in breaking strength efficiency is also about 1-2 % in small diameter cables. It can be seen from Tables 2 and 3 that increasing the cable size to 7 ϕ ×400 cannot be considered as a factor greatly influencing the breaking strength.

c) Scattering of elongation performance of wires

The breaking elongation of the wire is specified to be greater than 4 %⁸⁾ while the values actually measured were about 6 %, scattering from 5 % to 7 %. The actual breaking elongation of a cable where the amount of slippage was large (cases 1 and 2) was below the value of 4 % specified for the single wires. Although the cable consists of wires with the elongation performance mentioned, the reason for this reduction in the breaking elongation of a cable may be attributed not to a scatter in the mechanical properties of the wires, but to phenomena occurring as failure takes place in the socket as mentioned in a) above.

d) Effect of heat when casting the zinc-copper alloy

The temperature of the molten zinc-copper alloy during casting in the socket is about 460°C⁷⁾. It is generally thought that this heat may reduce the strength of the wires. However, from the results of the tensile breaking tests on large diameter cables, it can be seen that the effect of heat on the strength may be extremely small.

Thus far, consideration has been given to factors which affect the cable breaking strength. The most significant factor was found to be that associated with phenomena during socket failure.

4. ANALYSIS OF THE AMOUNT OF SLIPPAGE IN THE ZINC-COPPER ALLOY

(1) Purpose of the analysis

It has been determined that the largest factor affecting cable breaking strength efficiency and the failure

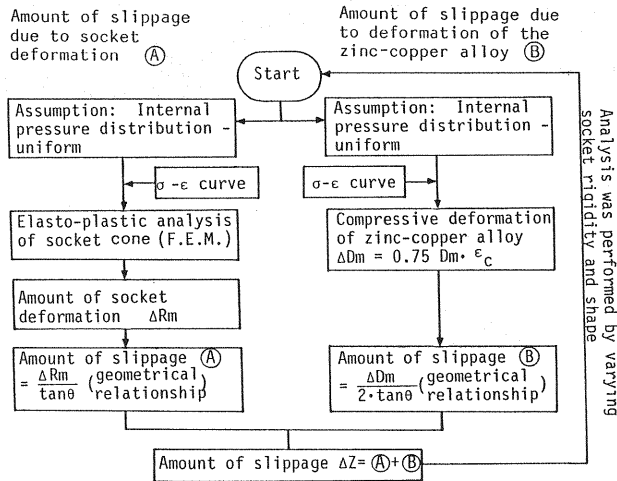


Fig.5 Analytical flow for amount of slippage.

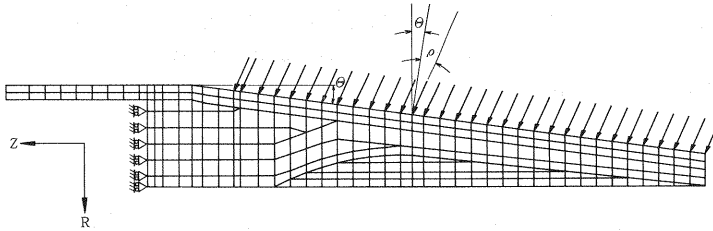


Fig.6 F.E.M. model (Thick walled front-bearing type).

pattern is the fact that a large amount of slippage occurs and the cause of this is lack of socket rigidity t_m/D_m . The amount of slippage is now calculated analytically, taking socket rigidity t_m/D_m , the type of the socket, and the yield stress of the socket material as parameters. And consideration is also given to the value of socket rigidity t_m/D_m necessary to control the slippage. The aim of this analysis is to create a new design method for large sockets that takes into account the ultimate strength.

(2) Summary of the analysis

An elasto-plastic analysis of the amount of slippage was carried out by considering the total slippage as the sum of a component due to socket deformation and a component due to compressive deformation of the zinc-copper cone. The analytical flow is shown in Fig.5.

D_m is the mean variation in diameter of the zinc-copper cone and R_m is the variation in internal radius of the socket at the same position. θ is the taper angle of the internal socket face.

The stress-strain curves for the socket material and for the zinc-copper alloy, which are required in this analysis, were obtained by material tests.

The socket cone was analyzed using an elasto-plastic analysis by the Finite Element Method in which the socket was modelled as an axially symmetrical element and the load obtained by Eq. (4) was taken as the equivalent nodal point load. Fig.6 shows F.E.M. model example. After obtaining the socket deformation R_m , the slippage (A) was calculated by Eq. (5) shown in Fig.5, which is based on the geometry of the internal face of the socket.

$$P = \frac{T}{A} \cdot \frac{1}{\sin(\theta + \rho)} \quad (4)$$

$$(A) = \frac{\Delta R_m}{\tan \theta} \quad (5)$$

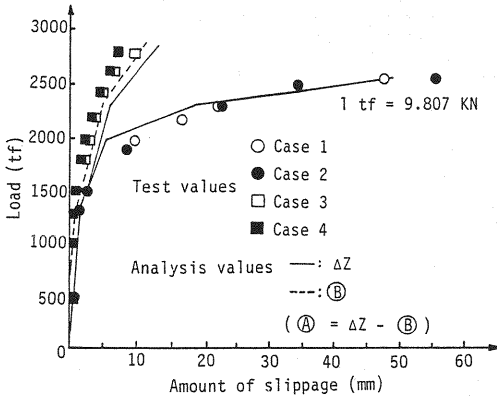


Fig. 7 Relationship between load and slippage in the front-bearing type of socket (7 $\phi \times 421$).

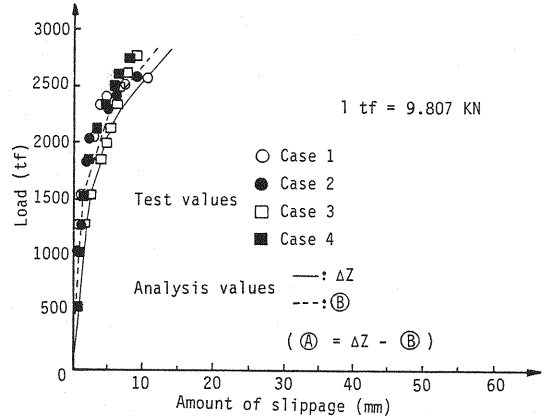


Fig. 8 Relationship between load and slippage in the rear-bearing type of socket (7 $\phi \times 421$).

Next, the compressive strain ϵ_c in the zinc-copper alloy cone was obtained by substituting the internal pressure σ_m , obtained by Eq. (1) into the compressive stress-strain curve for the zinc-copper alloy which is independent of the socket type and its deformation. Although the strain ϵ_c in the zinc-copper alloy is under three-axis stress, a nearly accurate ΔD_m value is obtained. And the amount of compressive deformation ΔD_m was then calculated by Eq. (6).

$$\Delta D_m = 0.75 D_m \cdot \epsilon_c \dots \dots \dots (6)$$

Where, D_m : Mean diameter of zinc-copper alloy, ϵ_c : Compressive strain (%) in zinc-copper alloy cone, 0.75 : Ratio of area of zinc-copper alloy only to the cross sectional area of the cone at the point where D_m is defined (The ratio is 0.75 for almost all sizes and analysis of ΔD_m using this value well agrees with the measured slippage in each case).

The slippage \textcircled{B} was calculated by Eq. (7) (based on the geometrical relationship) from the deformation ΔD_m in mean diameter D_m .

$$\textcircled{B} = \frac{\Delta D_m}{2 \cdot \tan \theta} \dots \dots \dots (7)$$

The slippage in the zinc-copper alloy cone ΔZ is the sum of the values obtained in Eqs. (5) and (7). As shown in Figs. 7 and 8, the results of this analysis correlate well with the actually measured values, verifying the accuracy of this method of analysis.

It can be seen that in the case of the thin walled front-bearing type of socket (cases 1 and 2 in Fig. 7) the total slippage in the zinc-copper alloy cone, ΔZ , is dominated by slippage due to the large socket deformation \textcircled{A} , while in the case of the thick walled front-bearing type of socket (cases 3 and 4 in Fig. 7) and the rear-bearing type of socket (cases 1-4 in Fig. 8) it is clear that the total slippage is extremely small and a greater contribution to ΔZ comes from the deformation of the zinc-copper alloy cone \textcircled{B} .

(3) Results of analysis

Fig. 9 shows the results of theoretical analysis on the front-bearing type and rear-bearing type which have been applied for many bridges, in addition, a back-fixed type for case study, when the yield stress of the socket material is $\sigma_y = 42 \text{ kgf/mm}^2$ (412 MPa). In the case of the front-bearing type, it can be seen that the slippage rapidly increases as the rigidity of the socket, t_m/D_m , drops below 0.22-0.23, and the rigidity of the thin walled front-bearing type of socket designed by the conventional method is apparently insufficient at the ultimate strength because t_m/D_m is 0.165.

In the case of the rear-bearing type, the relationship between the rigidity t_m/D_m of the socket and the amount of slippage is insignificant. And in the case of back fixed type, the amount of slippage does not increase markedly even though the rigidity is relatively small. The reason for this may be that the hoop

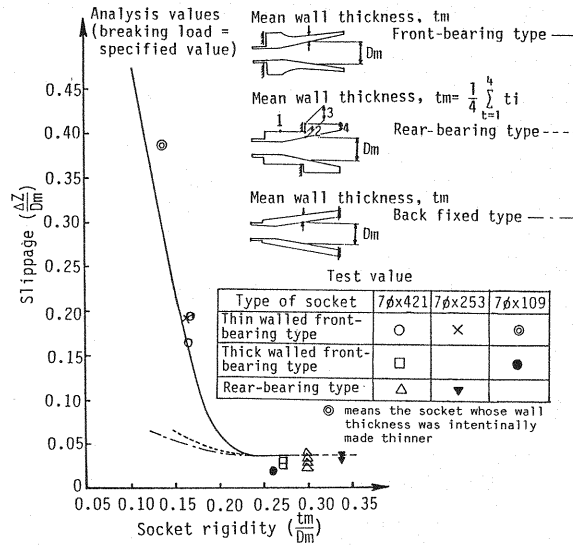


Fig. 9 Amount of slippage by socket rigidity and bearing type.

stress and the axial stress which are both positive, have a sufficient yield condition and so the amount of deformation is controlled.

Accordingly, it is particularly important to design the socket with adequate rigidity when the extensively used front-bearing type of socket is considered.

Next, the relationship between the load and slippage in the zinc-copper alloy cone (a curve similar to Fig. 9) was studied when θ is 7.5° and ρ is 16.7° in Eq. (1). These two values are well used for sockets secured with zinc-copper alloy. Table 4 shows the values of socket rigidity that are able to restrict the slippage to small values at the ultimate condition (the specified value of cable breaking load). The fact that these values are not seriously affected by the bearing position in each type was also confirmed using a similar process.

Table 4 Required rigidity of socket.

Type \ σ_y	42 kgf/mm ²	37 kgf/mm ²	32 kgf/mm ²
Front-bearing type socket	$t_m/D_m \geq 0.22$	$t_m/D_m \geq 0.25$	$t_m/D_m \geq 0.30$
Rear-bearing type socket	$t_m/D_m \geq 0.19$	$t_m/D_m \geq 0.21$	$t_m/D_m \geq 0.25$
Back fixed type socket	$t_m/D_m \geq 0.16$	$t_m/D_m \geq 0.18$	$t_m/D_m \geq 0.21$

1 kgf/mm² = 9.807 MPa

5. STUDY ON A NEW DESIGN METHOD FOR LARGE SOCKETS

(1) Summary of the design method

This new method of design for socket cone requires two calculation, a) and b), to overcome the limitations associated with the conventional design method previously mentioned. In this new method, the length of the alloy cone is calculated by the conventional method. When designing a socket of larger dimensions, its length is determined by Eq. (1).

Fig. 10 shows the analytical flow for the new method of design for large sockets when the breaking load of cable is greater than about 1 000 tf (9 800 kN).

a) Checking the stress at the cable design load

The cable design load means the load obtained by multiplying the cross-sectional area of the cable by the allowable stress of each wire. While the conventional design method considers only the hoop stress, this new method takes into account the axial stress, the radial stress occurring in the socket and the hoop stress, thus checking the combined stress, using Eqs. (8) and (9).

$$\sigma_{eq} = \frac{1}{\sqrt{2}} \sqrt{(\sigma_r - \sigma_\theta)^2 + (\sigma_\theta - \sigma_z)^2 + (\sigma_z - \sigma_r)^2} \dots \dots \dots (8)$$

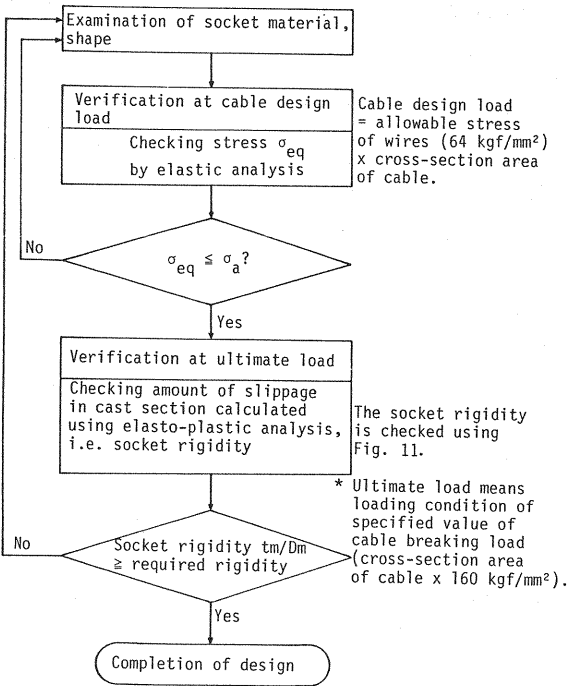


Fig.10 Large socket design method.

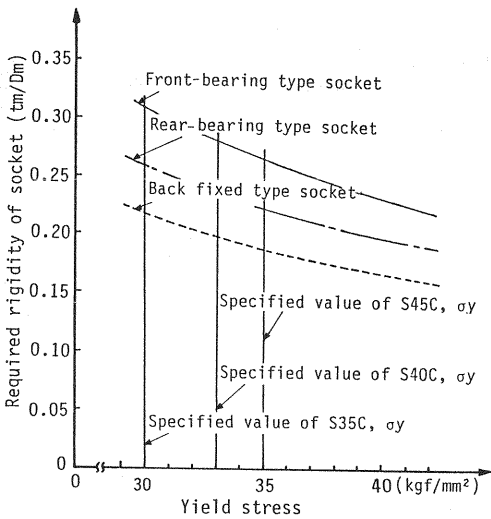


Fig.11 Relationship between the yield stress and required socket rigidity (breaking load : specified value).

Where, σ_r : Radial stress, σ_θ : Hoop stress, σ_z : Stress in the axial direction,

$\sigma_{eq} \leq \sigma_a$ (9)

Where, σ_a : Allowable stress of the socket cone

b) Checking the socket rigidity at the ultimate strength

The ultimate strength means the condition defined by the specified value of cable breaking load. In order to restrict the amount of slippage in the zinc-copper alloy cone at the ultimate strength to a small value, the concept of rigidity t_m/D_m is introduced. This check can be done using Fig. 11, which is Table 4 presented in graphical form, and the socket rigidity should not fall below the required value at the yield stress (specified value) of the socket material.

(2) Application of the new design method

This new design method is exemplified for the case of a front-bearing type of socket, the most extensively used.

The stress should be checked at the mid-point ($l/2$) of the zinc-copper alloy cone as shown in Fig. 12. After calculating the internal pressure, σ_M , using Eq. (1), three values of stress are calculated, as follows :

a) Hoop stress

The maximum value σ_θ occurs on the internal face of the socket, and it can be calculated from Eq. (3) for a thick walled circular pipe.

b) Radial stress

The maximum value σ_r occurs on the internal face of the socket, and it can be calculated using Eq. (10).

$\sigma_{r\max} = -\sigma_M$ (10)

c) Stress in the axial direction σ_z

Considering the apportionment of axial force at the mid-point ($l/2$) of the zinc-copper alloy cone, the compressive force in the hatched section of Fig. 12 is borne by the cross-sectional area of the socket cone, σ_z can be calculated from Eq. (11).

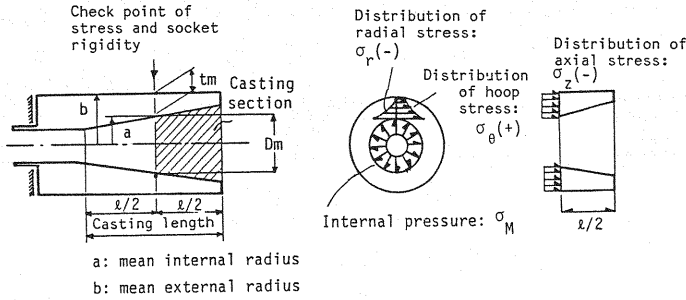


Fig.12 Position for checking stress and rigidity.

$$\sigma_z = -\frac{1}{\pi(b^2 - a^2)} \cdot \frac{A'}{A} \cdot T \dots \dots \dots (11)$$

Where, A' : Contact area of zinc-copper alloy cone (hatched section) in Fig.12, A : Effective contact area of zinc-copper alloy cone, T : Cable design load, a : Internal radius of socket at the mid-point ($l/2$), b : External radius of socket at the mid-point ($l/2$).

Since σ_θ , σ_r and σ_z above are obtained independently by disregarding Poisson's effect, there may be a certain lack of strictness. But when compared with the results of elastic analysis using F. E. M. on the thick walled front-bearing type of socket given in Table 1, sufficient accuracy is clearly obtained for the purposes of practical application.

Next, the rigidity of the socket at the ultimate strength should not fall below the curve for the front-bearing type of socket shown in Fig.11. As an example, when this type of socket is manufactured from S45C the required rigidity t_m/D_m is 0.265, because the specified value of yield stress σ_y is 35 kgf/mm² (343 MPa). This is then the minimum value of rigidity t_m/D_m acceptable in the design.

The new design method was applied to the cable sockets used on the Yokohama Bay Bridge.

6. CONCLUSION

Thus far, the mechanical properties of large sockets secured with zinc-copper alloy and which are in extensive use, have been studied by tensile tests and analysis. Based on the results, a new method of design for large sockets has been developed which takes into consideration the ultimate strength.

The conclusions reached were as follows :

(1) When the conventional method of design is applied to a large socket, serious deformation occurs at the cable breaking load and the amount of slippage in the zinc-copper alloy is excessive. As a result, wire failures concentrate in one particular location in the socket and the breaking strength efficiency is reduced. The degree of reduction increases as the amount of slippage goes up.

(2) The reason for the phenomenon described above is that the conventional design method only considers the hoop stress, thus yielding a wall thickness susceptible to deformation.

(3) In the case of a thick-walled socket, the deformation and amount of slippage were extremely small and the breaking strength efficiency of the large diameter cable (7 ϕ ×400 wires) was about 100 % as in the case of a small diameter cable. The failures were scattered along the cable and did not concentrate inside the socket.

(4) In consideration of the fact that the mechanical properties of a socket are related to the wall thickness and the slippage, a method of analyzing the amount of slippage was devised and tested on various socket types. As a result, it was found analytically that sockets based on the conventional method of design do not necessarily provide sufficient anchorage at the ultimate strength. In addition, a value of socket rigidity t_m/D_m which minimizes the amount of slippage was indicated.

(5) Based on the results of the analysis in (4) above, a new design method for large scale sockets

that guarantees anchorage at the ultimate strength was studied. The socket rigidity, t_m/D_m , which is not considered in the conventional method, was introduced and the rigidity was found to supply sufficient anchorage at the cable breaking load (specified value). In addition, a check of combined stress replaces the conventional consideration of only the hoop stress at the design load of the cable.

7. ACKNOWLEDGEMENTS

In closing, we would like to express our particular thanks to Mr. Noboru Tomita of Mitsubishi Heavy Industries, Ltd., and Mr. Nobuo Watanabe of NKK for their instructive advice during the course of this study.

REFERENCES

- 1) Japan Road Association : Specifications for Highway Bridges (JSHB), Feb., 1980.
- 2) JSSC : The Experimental Study on the Mechanical Behavior of the Anchor Socket, Vol.9, No.88, 1973.
- 3) JIS F 3482 Socket for Ships, 1968.
- 4) Eya, S., Takano, H. and Sakamoto, Y. : Mechanical Properties of Large Cable Sockets, 43th Annual Conference of JSCE, I-224, October, 1988 (in Japanese).
- 5) Tawarayama, Y. *et al.* : Structural Characteristics of NEW PWS for Cable-Stayed Bridges, Nippon Steel Technical Reprt No. 37, April, 1988.
- 6) Ougi, K. *et al.* : Hakai Kyodo Gaku, Ohmsha Ltd., pp.147-149, 1985.
- 7) JSSC : Standards for Structural Cables, Vol.14, No.149, 1978.
- 8) Honshu-Shikoku Bridge Authority : HBS G 3501-1979, June, 1979.

(Received August 29 1989)